Master's Thesis of Engineering

Compensation Pixel Circuits for Stretchable AMOLED Displays

스트레처블 AMOLED 디스플레이를 위한 픽셀 보상 회로

August 2023

Graduate School of Engineering
Seoul National University
Electrical and Computer Engineering Major

Jimin Kang

Compensation Pixel Circuits for Stretchable AMOLED Displays

지도 교수 이 수 연

이 논문을 공학석사 학위논문으로 제출함

2023년 8월

서울대학교 대학원

전기정보공학부

강 지 민

강지민의 석사 학위논문을 인준함

2023년 8월

위 원 장 홍 용 택 (인)

부위원장 이 수 연 (인)

위 원 곽 정 훈 (인)

Abstract

Recently, stretchable displays that can freely change their shape and size have been attracting attention as the ultimate form of deformable displays. Research on stretchable displays has mainly focused on finding ways to ensure stable operation even under mechanical stress. One of the widely used approaches is utilizing rigid-island structure that can buffer the strain directly applied to the display devices. Even if this structure can minimize the degradation of display images caused by display stretching, image quality problems in stretchable displays still exist. Since the luminance of the display is inversely proportional to the pixel area, so as the display expands, the pixel area increases, leading to a decrease in brightness.

Flat-panel active-matrix organic light emitting diode (AMOLED) displays have long relied on compensation technologies to ensure uniform and high-quality images. Compensation pixel circuits can prevent the degradation of image quality by compensating for the threshold voltage variation of the driving thin-film transistors (TFT).

In this paper, novel compensation pixel circuits for a stretchable AMOLED display with a rigid-island structure were proposed. The proposed pixel compensation circuits not only can effectively compensate for the threshold voltage variation of the driving thin-film transistors, but also address the issue of luminance reduction caused by display stretching through the introduction of a capacitive-type strain sensor. The proposed circuits utilize the linear relationship between the sensor and the strain to compensate for the luminance reduction. This approach offers a promising solution to enhance the image quality degradation problem in stretchable displays.

The operation and the compensation error rates of each pixel circuit are demonstrated by the SPICE simulation. The error rates caused by threshold voltage variation appear less than 10% even under strain and the luminance reductions due to stretching were effectively

suppressed after compensation. Simulation results verify that the proposed pixel circuits effectively prevent the luminance reduction and degradation of display images by compensating for the threshold voltage variations and strain effect.

Overall, this paper introduces a new approach to solving the problems of stretchable displays, demonstrating the potential for improving image quality in stretchable AMOLED displays.

Keyword : Stretchable display, AMOLED display, pixel circuit, compensation, strain sensor, rigid-island structure
Student Number : 2021-29608

Table of Contents

Chapter 1. Introduction

1.1. Background

Displays are critical components of electronic devices such as smartphones and computers, providing visualized information to users by converting electrical signals into light. In recent decades, there has been a remarkable evolution in active-matrix display technologies. The active-matrix organic light-emitting diode (AMOLED) display technology has been a dominant technology in flat-panel displays due to its advantages, including fast response time, high contrast ratio, wide viewing angles, and not requiring backlight units. Moreover, there are now deformable displays that can change their shape and size, pushing the boundaries of what is possible in terms of display technology.

Since the luminance of OLEDs is determined by the current, a thin-film transistor (TFT) is connected to the OLED to regulate the current flows into the OLED. As a result, the electrical properties of TFTs play a crucial role in display driving. While the oxide semiconductor-based TFTs, such as indium-gallium-zinc oxide (IGZO) TFTs, offer excellent electrical characteristics, their threshold

voltage can be significantly influenced by external stress and fabrication process fluctuation. This threshold voltage variation can degrade image quality and the uniformity of displays.

As the free-form properties of displays have been recognized as the leading future display technology, the development of deformable displays, including flexible, foldable, rollable, and stretchable displays, has gained significant attention. These displays offer possibilities for applications in various fields, from wearable to medical devices. Among them, stretchable displays, which can be bent or stretched in all directions without losing their functionality, have been nominated as the ultimate form of next-generation deformable displays.

However, since the electrical properties of conventional display devices are easily degraded by mechanical stress, unique technologies are needed to be developed for stretchable displays. One of them is adopting rigid-island structures that can protect the display devices from strain. However, even though rigid-island structures ensure stable operation under strain, the image quality issues in the stretchable displays still exist due to the threshold voltage variation of TFT and the luminance reduction that is inevitably caused by the stretching of the panel size.

In this thesis, compensation pixel circuits for stretchable AMOLED displays have been proposed. The proposed circuits utilize the capacitive-type strain sensor to detect and compensate for the strain effect. The source-follower method is exploited to compensate for the threshold voltage of oxide semiconductor-based TFT whose threshold voltage is usually less than 0 V. Through SPICE simulation results, it was shown that the proposed circuits effectively prevent image quality degradation in stretchable displays by compensating for both threshold voltage variation and strain effect.

1.2. Outline of This Thesis

An explanation of the pixel structures of AMOLED displays and stretchable displays is provided in Chapter 2. The chapter covers the basic pixel circuits and the compensation methods of AMOLED displays. The major issue and one of the solutions for the stretchable displays are also introduced in this chapter.

Chapter 3 focuses on the issue of luminance reduction in stretchable displays and explains the principle of stretchable display compensation. Additionally, the strain sensor that is used for the proposed compensation pixel circuits is introduced.

In Chapter 4, the proposed compensation pixel circuits for stretchable AMOLED displays are introduced. All the pixel circuits can compensate for both threshold voltage variations and the strain effect utilizing the principle explained in Chapter 3. The chapter provides detailed explanations of the operations of the proposed circuits, along with the SPICE simulation results.

The summary of the results is represented in Chapter 5, including a concise overview of the key findings of this thesis. Appendix A proposes the structure and the fabrication process of the IGZO TFTs used in SPICE simulations.

Chapter 2. Review of Display Technology

This chapter provides a comprehensive review of AMOLED display, with a focus on the basic pixel circuit structure and compensation pixel circuits. Furthermore, the chapter reviews developments in stretchable display technologies, which allow displays to maintain stable operation under mechanical stress.

2.1. Review of AMOLED Display

2.1.1. AMOLED Pixel Circuit

Since OLEDs are current-driven devices, the luminance of an OLED should be regulated by current density. Thus, most OLED pixel circuits have a driving thin-film transistor whose source node is connected to the anode of an OLED [1-2]. This configuration is used to control the current that flows into the OLEDs and hence their luminance.

As for driving TFTs, oxide semiconductor-based TFTs are commonly used. In the early 2000s, amorphous oxide semiconductors, such as IGZO, attracted attention as a novel semiconductor material

for the TFT channel [3-5]. The large bandgap of the oxide semiconductor results in significantly low leakage current making them suitable for large-sized displays. The overlapped 5s orbital among metal cations in oxide semiconductors is responsible for high field effect mobility around $10\ cm^2/V \cdot s$, and the amorphous phase of oxide semiconductor allows for good uniformity. Furthermore, low-cost and low-temperature fabrication processes enable oxide semiconductors to be a promising candidate.

Fig. 2-1. shows the simplest pixel circuit structure and operation for AMOLED displays consisting of 1 driving TFT (T1), 2 switching TFTs (T2, T3), and 1 storage capacitor (Cs). The cathode of the OLED is connected to the source node of T1, and the current density of the OLED can be controlled by applying data voltage to the gate node of T1.

When the n^{th} line addressing starts, T2 and T3 are turned on, so that the data voltage (V_{data}) comes through T2, charging Cs capacitor. At the end of the n^{th} line addressing, T2 and T3 are turned off to maintain V_{data} stored in Cs. Thus, the OLED can constantly emit light until the next frame time. The OLED current (I_{OLED}) can be expressed as the following equation:

$$I_{OLED} = \frac{1}{2}\mu C_{ox}\frac{W}{L}\left(V_{gs} - V_{th}\right)^2 \quad (2\text{-}1)$$

where μ, C_{ox}, W, L refer to mobility, oxide capacitance, width, and length of T1, respectively. V_{gs} is the voltage difference between the gate and the source node of T1, and V_{th} is the threshold voltage of T1.

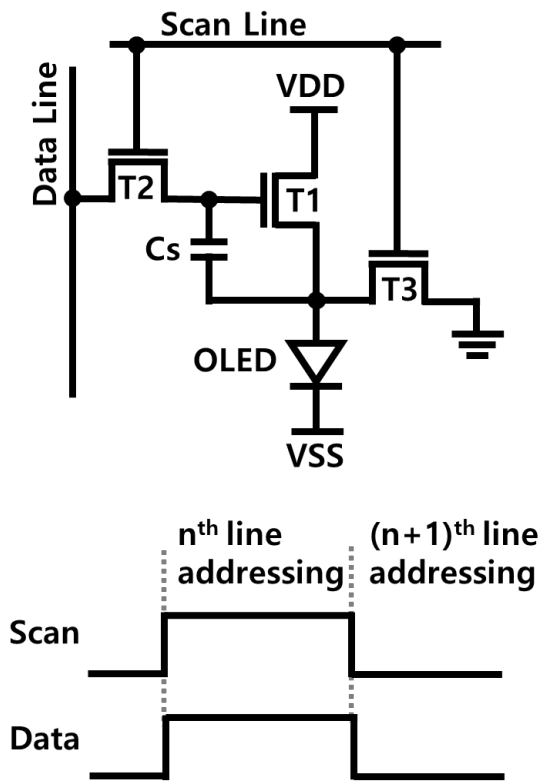

Fig. 2-1. The schematic of a basic 3T1C pixel circuit for AMOLED displays.

2.1.2. Display Compensation Technologies

The electrical properties of TFTs are key to determining the OLED current and the luminance of the pixel. However, the threshold voltage or mobility of TFTs can easily be varied by external stress, such as voltage bias or temperature change. Furthermore, the variation among TFTs that occurs during the fabrication process eventually degrades the uniformity of display images. For these reasons, compensation is necessary to achieve high quality and high reliability of displays [6-7].

So far, various technologies have been studied to compensate for V_{th} variations of driving TFTs. One of them is to exploit the compensation pixel circuits [8-10]. The compensation pixel circuits in each pixel sense and compensate for the threshold voltage of a driving TFT at the beginning of every addressing time. The designs of the compensation pixel circuits are divided into two types depending on the threshold voltage compensation method: the diode-connection method and the source-follower method.

Fig. 2-2(a). shows the simplest pixel circuit structure and operation principles of the diode-connection method. As shown in the figure, the gate and the drain nodes of the driving TFT are connected.

At the reset stage, the source node is set to V_{ref}, whereas the gate node is set as VDD. Then, the current flows through the driving TFT until the source node voltage increases as $VDD - V_{th}$. Thus, at the end of the compensation stage, V_{th} of the driving TFT is stored in the storage capacitor. When the stored V_{th} is added to data voltage (V_{data}) through additional switches and control signals, the voltage difference between the gate and source node voltage of driving TFT becomes $V_{data} + V_{th}$, so that the equation (2-1) can be rewritten by follows:

$$I_{OLED} = \frac{1}{2}\mu C_{ox}\frac{W}{L}(V_{data} + V_{th} - V_{th})^2 = \frac{1}{2}\mu C_{ox}\frac{W}{L}(V_{data})^2 \qquad (2-2)$$

As V_{th} of the driving TFT is canceled out in the equation, the OLED current is no longer affected by the variation of V_{th}.

As shown in Fig. 2-2(b), there is no connection between the drain and gate nodes of the driving TFT in the source-follower method. At the reset stage, the gate and source node of the driving TFT is set as V_{ref1} and V_{ref2}, respectively. When the compensation starts, the current flows, until the V_{th} of the T1 is stored in the storage capacitor. In the diode-connection method, since the gate node voltage is charged as VDD, the source node voltage cannot exceed the gate node voltage. Thus, the negative threshold voltage cannot be stored in the capacitor. On the other hand, in the source-follower method, the

source node voltage can increase over the gate node voltage (V_{ref1}). Therefore, the threshold voltage lower than 0 V can be stored in the source-follower method. Given most of the oxide TFTs have a threshold voltage lower than 0 V, the source follower method must be utilized for the pixel circuit to exploit such depletion-mode devices.

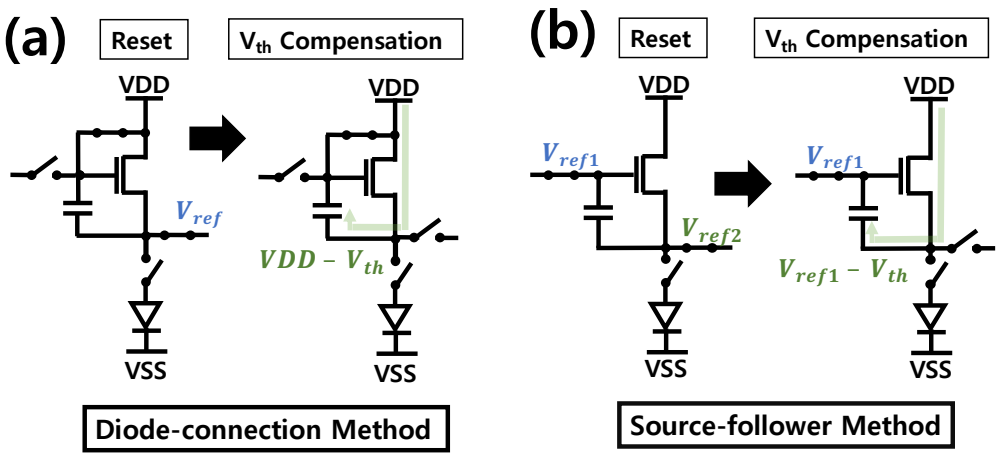

Fig. 2-2. The schematic and the simple V_{th} sensing principle of (a) diode-connection method and (b) source-follower method.

2.2. Review of Stretchable Display Technology

One of the major challenges for such deformable displays, including stretchable displays, is ensuring stable operation under strain [11-13]. Conventional display devices, such as thin-film transistors and OLEDs, are easily degraded by external mechanical stress, causing significant issues in display driving and image quality. To address these issues, two strategies are primarily employed: material-based approaches and structural approaches.

From a material-based perspective, research has focused on developing materials to fabricate devices that have intrinsic stretchability. In general, novel materials such as carbon nanotubes (CNT) and silver nanowires (AgNW) are commonly used to provide both stretchability and conductivity to metal electrodes, transistors, or light-emitting devices [14-16]. However, these devices often show low performance and energy efficiency compared to the devices used in conventional flat panel displays.

Another approach to achieve stretchability in a display without degradation of display devices is to adopt a special structure that can protect display devices from the strain applied to the display panel. The rigid-island structure is one of the most advanced technologies

among stretchable display structures [17-19]. As shown in Fig. 2-3, pixel elements such as TFTs and OLED are placed on rigid-island structures, which are mounted on the stretchable panel. These islands can be fabricated by polyimide or silicon patterning and connected by intrinsically stretchable interconnections [20-21]. Since Young's modulus of interconnections is much smaller than the rigid island, most of the modifications occur in the interconnections [22-23]. Thus, when the panel is stretched, only the lengths of the interconnections increase, ensuring that the display devices mounted on the rigid islands remain unaffected by external stress. By exploiting the rigid-island structure, it is expected to be able to mass-produce stretchable displays suitable for various applications.

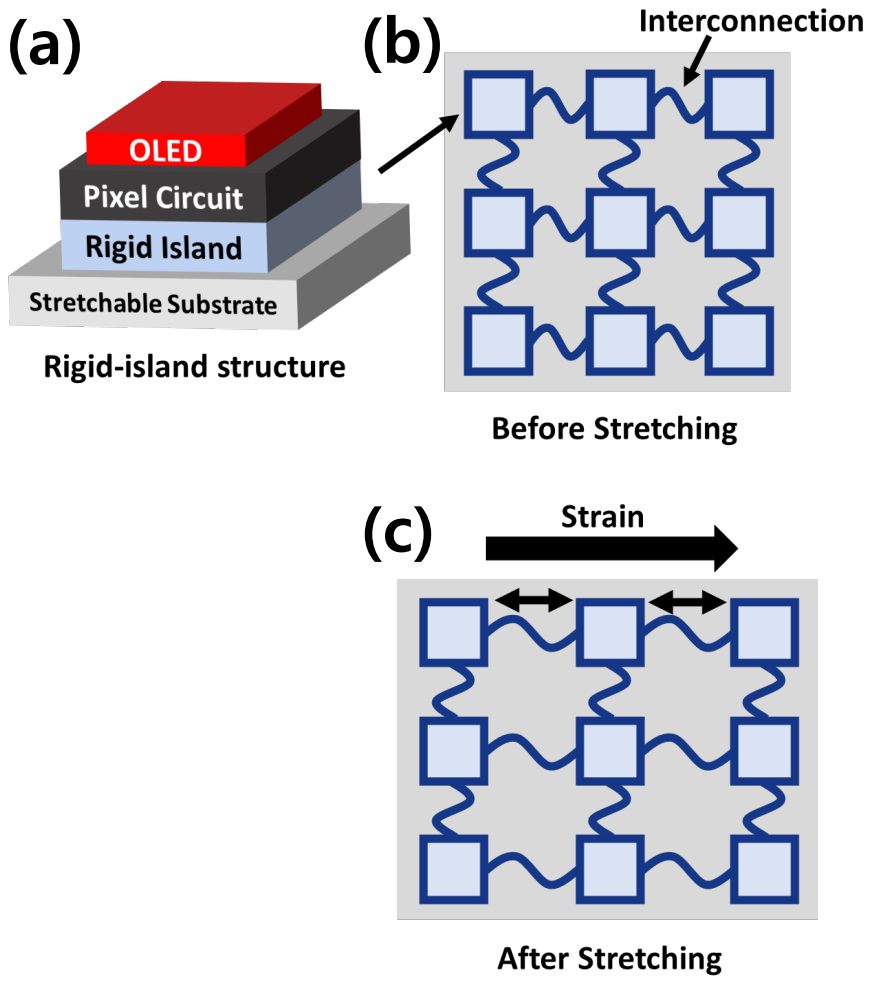

Fig. 2-3. (a) The schematic of rigid-island structure and plan view of rigid-island structure stretchable display (b) before and (c) after stretching

Chapter 3. Principle of Strain Effect Compensation

This chapter delves into the image quality degradation issue of stretchable displays caused by the stretching of the display panel and proposes a compensation principle to address it. The chapter begins with an introduction to the issue of luminance reduction in stretchable displays. Then, the strain sensor, which can detect and compensate for strain in the proposed pixel circuits, is explained in detail. Finally, the circuit structure for strain effect compensation and operation principle is proposed.

3.1. Luminance Reduction in Rigid-island Structure Stretchable Displays

As explained in the previous chapter, the rigid-island structure provides protection to the pixel circuits and light-emitting devices from mechanical strain applied to the display panel. Although the rigid-islands can prevent the degradation of electrical properties of pixel elements from strain, they may not necessarily address all

display image quality issues.

In general, the luminance of the OLED display is proportional to the current flows into the OLED (I_{OLED}) and inversely proportional to the panel size (A). If the strain is not applied to the panel, the luminance (L_0) can be expressed by following equation (3-1).

$$L_0 = \eta \frac{I_{OLED}}{A} \tag{3-1}$$

where η is the OLED current efficiency.

Assume that a stretchable display with a length of l and a width of w is constructed using rigid-island structures, and that the electrical properties of pixel devices, such as threshold voltage and mobility of TFTs and OLEDs, remain unaffected. When a strain ϵ is applied on the stretchable display panel, l would increase by a factor of $(1+\epsilon)$, while w would decrease by $(1-\nu\epsilon)$ times, where ν is a Poisson's ratio of the stretchable display panel. Consequently, the area of the display panel expands by a factor of $(1+\epsilon)(1-\nu\epsilon)$. Thus, the display luminance after stretching (L) would inevitably decrease by a factor of $(1+\epsilon)(1-\nu\epsilon)$, which we will refer to as 'luminance reduction' throughout this paper.

$$L = \eta \frac{I_{OLED}}{A(1+\epsilon)(1-\nu\epsilon)} \tag{3-2}$$

To handle these problems, novel pixel circuits are proposed to compensate for the strain effect to decrease luminance reduction. The proposed circuits increase I_{OLED} by $(1+\epsilon)(1-\nu\epsilon)$ times, so that the luminance becomes the same as before stretching. These strain compensation principles are well illustrated in Fig. 3-1.

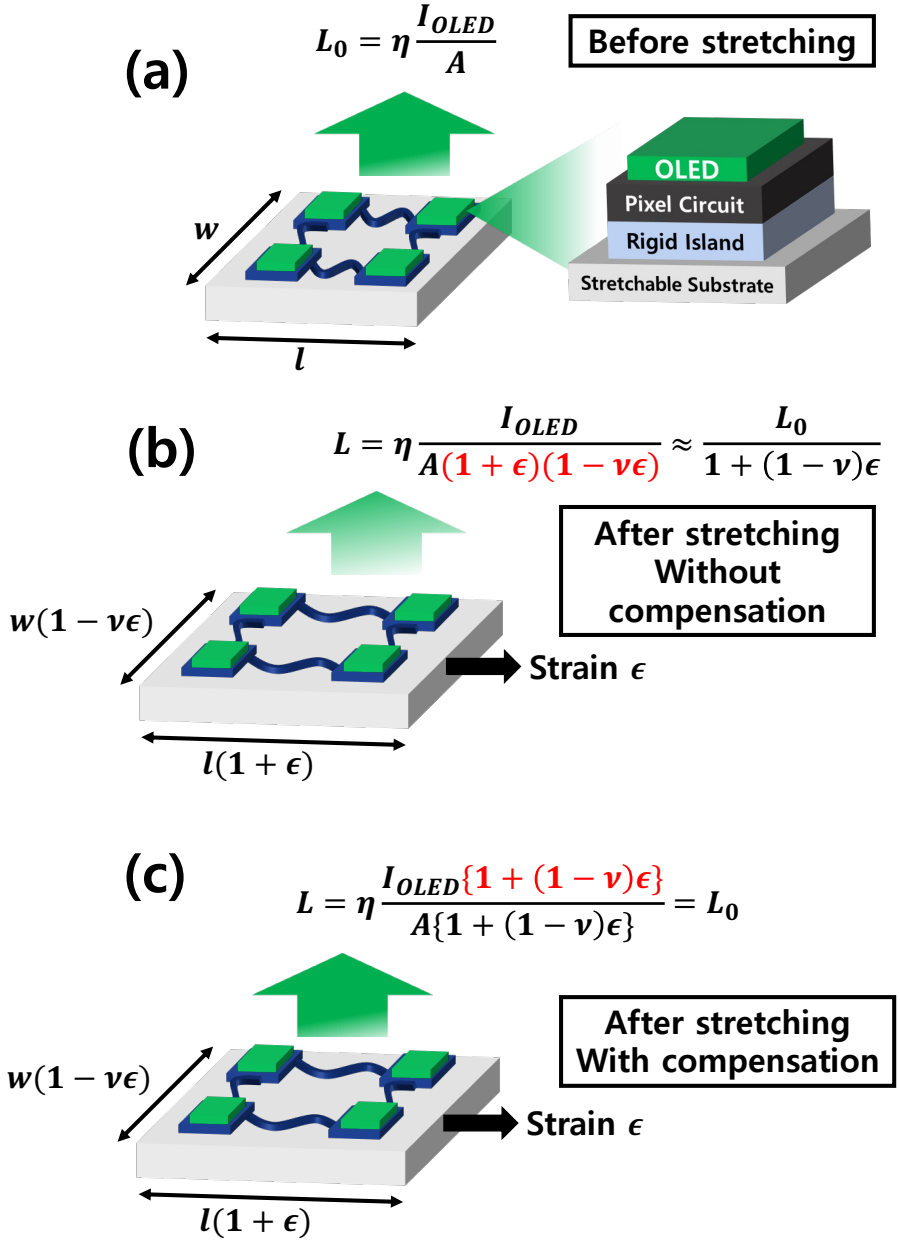

Fig. 3-1. The strain compensation principles of stretchable display (a) before stretching (b) after stretching without compensation and (c) with compensation.

3.2. Strain Sensor

In this work, compensation pixel circuits for stretchable displays have been proposed to compensate for the strain effect. The proposed circuits adopt a capacitive-type strain sensor that can sense and compensate for the strain applied on the stretchable display panel.

Strain sensors, which transform mechanical strain into electrical signals, are crucial components for stretchable electronics and have been adopted in diverse applications, such as medical devices and soft robotics [24]. Various types of strain sensors using different materials and structures have been developed to be applied in different fields, from wearable display devices to medical applications.

Strain sensors can be categorized into different types based on their features and operating mechanism, with the resistive-type and capacitive-type being the most common. The resistive-type strain sensor detects changes in its resistance for the detection of strain [25-26]. In general, resistive-type strain sensors are composed of the integration of stretchable and conductive materials such as CNT or graphene [27-28]. When the strain is applied, the geometric characteristics of the sensor, such as length and width, or the intrinsic structure are deformed, resulting in a change of resistance. The

sensitivity of strain sensors varies according to the materials and structure used, and they typically exhibit a non-linear response to strain.

On the other hand, capacitive-type strain sensors detect the strain through changes in capacitance [29-30]. These sensors have a soft insulator sandwiched between two flexible electrodes. When the initial width and length of the sensor are w_s and l_s, and the permittivity and thickness of the insulator are ε and d_s, respectively, the initial capacitance of the sensor (C_{s0}) can be expressed as the following equation:

$$C_{s0} = \varepsilon \frac{w_s l_s}{d_s} \tag{3-3}$$

When the strain (ϵ) is applied to the sensor along the width, w_s increases to $w_s(1+\epsilon)$, while both length and thickness of the sensor decrease by $(1-\nu_s\epsilon)$ times, where ν_s refers to the Poisson's ratio of the sensor. Thus, the capacitance of the sensor with applied strain (C_s) will be described as the following equation:

$$C_s = \varepsilon \frac{w_s(1+\epsilon) l_s(1-\nu_s\epsilon)}{d_s(1-\nu_s\epsilon)} = \varepsilon \frac{w_s(1+\epsilon) l_s}{d_s} = C_{s0}(1+\epsilon) \tag{3-4}$$

As shown in the equation, the capacitance of the strain linearly increases as the applied strain increases [31].

In this work, the linear relationship between the capacitance of the sensor and the strain is utilized to detect and compensate for the strain. Capacitive-type strain sensors could be located on the stretchable display panel without rigid-island structures, with each sensor connected to a peripheral pixel circuit mounted on a rigid-island. The sensor can be fabricated by the solution process, such as inkjet printing, utilizing the soft electrodes like silver and soft dielectric materials like polyimide [31]. The overall proposed concept of a stretchable display with a strain sensor is depicted in Fig. 3-2.

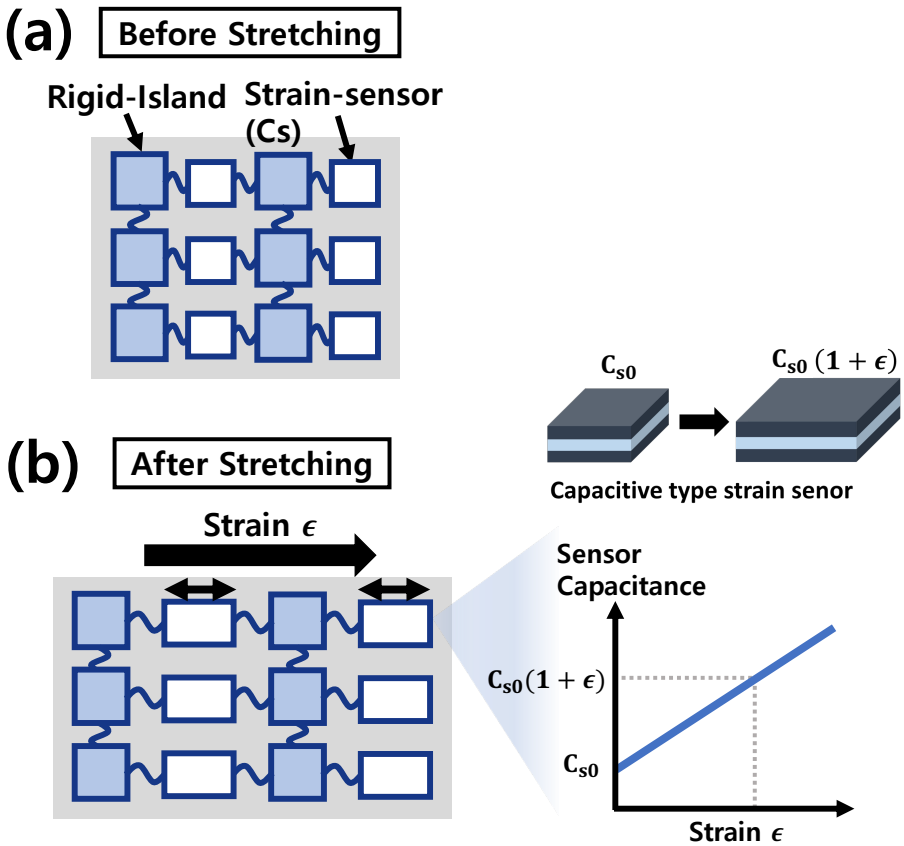

Fig. 3-2. The concept of the proposed stretchable display structure (a) before and (b) after stretching.

3.3. Circuit Structure for Strain Effect Compensation

Assume that there is no strain applied on the panel, and the capacitance of the sensor and capacitor are $\mathrm{C_s}$ and C, respectively. At the data input stage, the data voltage (V_{data}) comes through the cathode of the strain sensor and charges the sensor and capacitor. By the capacitive coupling of the sensor and capacitor, voltage of the node A can be expressed as $V_{data}\frac{\mathrm{C_s}}{\mathrm{C}+\mathrm{C_s}}$. Note that the node A, which is located between C and $\mathrm{C_s}$, is connected to the gate node of the driving TFT in the pixel circuit.

When the strain ϵ is applied, $\mathrm{C_s}$ increases by $(1+\epsilon)$ times, so the voltage of node A will change as the following equation.

$$V_{data}\frac{\mathrm{C_s}(1+\epsilon)}{\mathrm{C}+\mathrm{C_s}(1+\epsilon)} \tag{3-3}$$

If the strain ϵ is less than 1, the equation (3-3) can be approximated using Taylor expansion as follows:

$$V_{data}\frac{\mathrm{C_s}(1+\epsilon)}{(\mathrm{C}+\mathrm{C_s})\left(1+\frac{\epsilon \mathrm{C_s}}{\mathrm{C}+\mathrm{C_s}}\right)} \tag{3-4}$$

$$\approx V_{data}\left\{\frac{\mathrm{C_s}(1+\epsilon)}{\mathrm{C}+\mathrm{C_s}}\left(1-\frac{\epsilon \mathrm{C_s}}{\mathrm{C}+\mathrm{C_s}}\right)\right\} \approx V_{data}\left\{\frac{\mathrm{C_s}}{\mathrm{C}+\mathrm{C_s}}\left(1+\frac{\epsilon \mathrm{C}}{\mathrm{C}+\mathrm{C_s}}\right)\right\}$$

The Poisson's ratio of the panel is a constant value depending on the material properties. Thus, the following assumption can be

established by adjusting the capacitance value of the sensor and capacitor.

$$\frac{C}{C + C_s} = \frac{1 - \nu}{2} \tag{3-5}$$

For example, it is known that PDMS, a commonly used substrate material for stretchable display panel, have a Poisson's ratio of 0.5 [13]. In this case, the size of the capacitor and sensor should be adjusted so that C_s is three times larger than C.

By applying the equation (3-5), the equation (3-4) can be modified as follows:

$$V_{data}\left(\frac{C_s}{C + C_s}\right)\left\{1 + \frac{(1 - \nu)\epsilon}{2}\right\} \tag{3-6}$$

Since the Poisson's ratio ν is always less than 1, $\left\{1 + \frac{(1-\nu)\epsilon}{2}\right\}$ can be approximated to $\sqrt{1 + (1 - \nu)\epsilon}$. The node A is connected to the gate node of the driving TFT, so that V_{gs} of the driving TFT can be increased by $\sqrt{1 + (1 - \nu)\epsilon}$ times, increasing the I_{OLED} by a factor of $\{1 + (1 - \nu)\epsilon\}$.

As shown in the equation (3-2), we have verified that the luminance of the stretchable display decreases by $(1 + \epsilon)(1 - \nu\epsilon)$ times. Since both the strain ϵ and the Poisson's ratio ν are less than 1, this can be approximated to $\{1 + (1 - \nu)\epsilon\}$. The proposed circuits increase

I_{OLED} to $I_{OLED}\{1+(1-\nu)\epsilon\}$, so that the luminance becomes the same as before stretching. These strain compensation principles are well illustrated in Fig. 3-1.

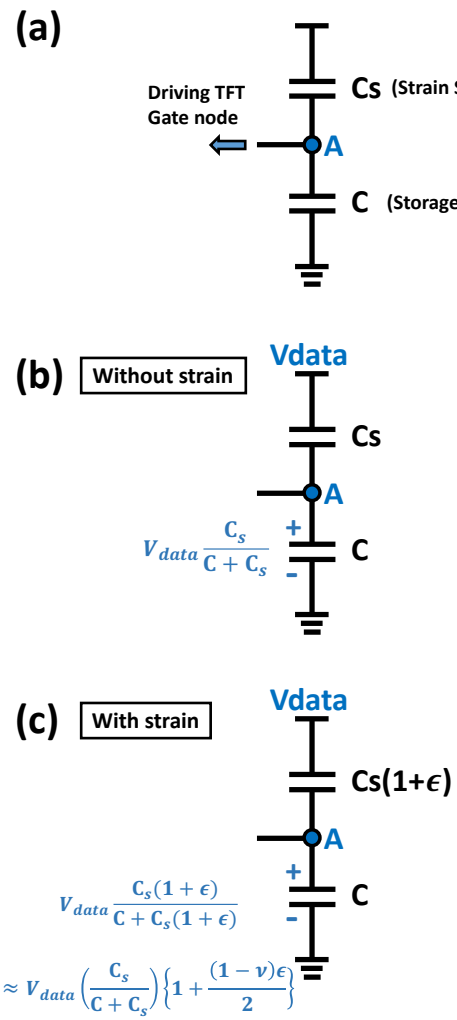

Fig. 3-3. (a) The circuit schematic of serial connection between a storage capacitor and a capacitive-type strain sensor and the operation (b) without and (c) with strain.

Chapter 4. Design of Stretchable Display Pixel Circuits

In this chapter, three proposed pixel circuits for stretchable displays are introduced. All the proposed circuits employ the principle of compensating for both threshold voltage and strain effect, which was explained in Chapter 3. Each of the proposed circuits has its own structure and circuit elements, resulting in different performance characteristics. The performance of each circuit is verified using SPICE simulation, which is presented in detail.

4.1. The Proposed 6T2C Pixel Circuit for Stretchable Display

4.1.1. The Operation Principle of the Proposed 6T2C Pixel Circuit

The schematic of the proposed 6T2C pixel circuit for stretchable display and the timing diagram of all signals are presented in Fig. 4-1. The pixel circuit comprises of 1 driving TFT (T1), 5 switching TFTs (T2 – T6), and two storage capacitors (C1, C2). The driving TFT features a double-gate structure, with the left-side gate referred to

as the first gate, and the right-side gate referred to as the second gate for ease of reference. C1 is connected between the first gate and the source node of T1, while C2 is connected between the second gate and the source node of T1. Additionally, the capacitive strain sensor (Cs) is connected in series with C2, which is the same circuit structure depicted in Fig. 3-3(a).

The operation of the pixel circuit is divided into four stages within one frame time: (A) reset, (B) V_{th} compensation, (C) data input, and (D) emission. The detailed operation at each stage is described as follows.

(A) Reset Stage

All the signals except for the EM are high, so all the switching TFTs are turned on except for T6. The OLED emission is not allowed since T6 is turned-off. The first gate, second gate, and source nodes are reset to V_{ref}, 0 V, and 0 V, respectively.

(B) V_{th} Compensation Stage

The S1 signal goes low to turn off T3 and T4. At the same time, the EM signal goes high to turn on T6, and the current starts to flow through T1 and charges the source node of T1. VSS is set to be higher than the source node of T1 to block the current flows into the OLED, so that At the end of this stage, V_{th} of T1 stored in C1. The second

gate of T1 maintains 0 V throughout this stage.

(C) Data Input Stage

After V_{th} compensation ends, the S1 goes high and the S2 and EM go low, so that T2 and T5 are turned off, and T3 and T4 are turned on. The data voltage (V_{data}) comes through T4 and charges C2 and Cs. At the same time, the source node of T1 is set to 0 V by T3. Due to the capacitive coupling, the voltage stored in C2 and Cs can be expressed as $V_{data}\frac{C_s}{C_s+C_2}$ and $V_{data}\frac{C_2}{C_s+C_2}$, respectively.

It is well known that the threshold voltage of double-gate structure IGZO TFTs can be modulated by the voltage between the second gate and source node (V_{gs2}) [32-34]. The relationship between V_{th} and V_{gs2} can be expressed as $V_{th} = -\alpha\Delta V_{gs2}$, where α is a coefficient which can be expressed by the following equation.

$$\alpha = -\frac{dV_{th}}{dV_{gs2}} = \frac{t_{gs1}}{\frac{\varepsilon_{gs1}}{\varepsilon_{IGZO}}t_{IGZO} + t_{gs2}} \quad (4-1)$$

where t_{gs1} is the first gate insulator thickness, t_{IGZO} is the IGZO channel thickness, t_{gs2} is the second gate insulator thickness, ε_{gs1} and ε_{IGZO} is the first gate oxide and IGZO dielectric constant, respectively.

Thus, the threshold voltage of T1 at this stage ($V_{th} + \Delta V_{th}$) can be described as follows.

$$V_{th} + \Delta V_{th} = V_{th} - \alpha \Delta V_{gs2} = V_{th} - \alpha \left(V_{data} \frac{C_s}{C_s + C_2} \right) \quad (4-2)$$

(D) Emission Stage

Finally, the S1 signal goes low and EM signal goes high, and the OLED starts to illuminate. V_{th} and $V_{data} \frac{C_s}{C_s+C_2}$ are stored in C1 and C2, respectively, so I_{OLED} can be expressed as following equation.

$$\begin{aligned} I_{OLED} &= k\{V_{gs1} - (V_{th} + \Delta V_{th})\}^2 \\ &= k\left[V_{th} - \left\{V_{th} - \alpha\left(V_{data}\frac{C_s}{C_s + C_2}\right)\right\}\right]^2 \\ &= k\left\{\alpha\left(V_{data}\frac{C_s}{C_s + C_2}\right)\right\}^2 \end{aligned} \quad (4-3)$$

where $k = \frac{1}{2}\mu C_{ox}\frac{W}{L}$ and V_{gs1} is the voltage between the first gate and source nodes of T1. Therefore, I_{OLED} is not affected by the threshold voltage variation.

By applying the equation (3-5), ΔV_{th} with strain ϵ will be described as follows.

$$\alpha\left\{V_{data}\frac{C_s(1+\epsilon)}{C_s(1+\epsilon)+C_2}\right\} \approx \alpha\left(V_{data}\frac{C_s}{C_s+C_2}\right)\left\{1+\frac{(1-\nu)\epsilon}{2}\right\} \quad (4-4)$$

In this case, the equation (4-3) is also changed as follows.

$$I_{OLED}\{1 + (1-\nu)\epsilon\} = k\left\{\alpha\left(V_{data}\frac{C_s}{C_s + C_2}\right)\sqrt{1 + (1-\nu)\epsilon}\right\}^2 \quad (4-$$

5)

Therefore, it is demonstrated that the proposed circuit can compensate for both the threshold voltage variation and the luminance reduction

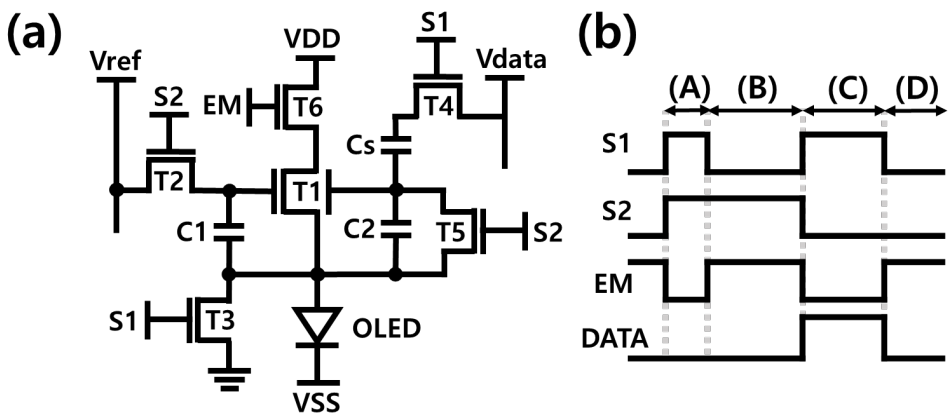

Fig. 4-1. (a) The schematic and (b) the timing diagram of control signals of the proposed 6T2C pixel circuit.

4.1.2. The Simulation Results

To verify the operation of the proposed pixel circuit, the Smart SPICE simulation was performed. The parameters of the level 62 Rensselaer Polytechnic Institute (RPI) TFT model were extracted by fitting the fabricated single-gate structure IGZO TFT. The V_{th} and mobility of the fabricated single-gate TFT were 0.83 V and 7.37

$cm^2/V \cdot s$, respectively. The fabricated and fitted transfer characteristics of IGZO TFT and the device structure are represented in Fig. 4-2(a). The double-gate structure property was implemented by Verilog-A in Smart SPICE and the results are depicted in Fig. 4-2(b). As shown in the inset of Fig. 4-2(b), as V_{gs2} increases with an interval of 1 V from -5 V to 5 V, the V_{th} of the curve shifts nearly 1 V. This verifies that the model successfully implements the double-gate structure properties. α was set close to 1, which can be achieved by setting 150 nm thick bottom and top gate insulator and 30 nm thick channel [35]. These are reasonable values for device fabrication. The design parameters and voltage levels used in the simulation are represented in Table 1. ν was set as 0.5, and the capacitance was adjusted in accordance to the equation (3-5).

Parameters	Value	Parameters	Value
$\left(\frac{W}{L}\right)_{T1}$	$\frac{12\ \mu m}{5\ \mu m}$	$\left(\frac{W}{L}\right)_{T2-T6}$	$\frac{5\ \mu m}{5\ \mu m}$
C1	300 fF	C2	100 fF
Cs	300 fF	Vref	3 V
VDD	20 V	VSS	2 V
VGH/VGL	20 V/−5 V	Data Voltage	0.5 V ~ 5 V

Table 1. The design parameters and voltage levels used in 6T2C circuit simulation.

The transient waveform of V_{data}, gates and source node voltage of T1 is presented in Fig. 4-3. Strain was neglected in this case. The V_{th} of T1 detected at the end of the V_{th} compensation stage (B) is maintained throughout the rest of the period. V_{gs2} at the data input stage (C) appears as 2.82 V, which is nearly identical to the value calculated by the equation (4-4). This value is preserved almost the same at the emission stage (D).

Fig. 4-4 shows the compensation error rate as a function of OLED current, when 0% and 15% strain is applied and V_{th} of T1 are shifted by ± 0.5 V. The error rate was calculated by following equation:

$$\frac{\left|I_{\Delta V_{th}=0} - I_{\Delta V_{th}=\pm 0.5}\right|}{I_{\Delta V_{th}=0}} \times 100\ (\%), \qquad (4\text{-}6)$$

where $I_{\Delta V_{th}=0}$ and $I_{\Delta V_{th}=\pm 0.5}$ refer to the OLED current when V_{th} are shifted by 0 V and ±0.5 V, respectively. The current error rates at 15% strain were simulated with the 15% increased capacitance of the sensor. As shown in the figure, the current error rates appear almost the same at 0% and 15% strain, and both are effectively suppressed to below 10% in all cases. The results verify that the proposed pixel circuit can compensate for the threshold voltage variations even when the strain is applied to the panel.

Fig. 4-5 depicts the simulation results of the luminance as a function of V_{data} before and after compensation. The luminance was calculated by the equation (3-1) with the simulated I_{OLED} values. Display stretching was implemented by increasing A by $(1+\epsilon)(1-\nu\epsilon)$ times. I_{OLED} were simulated with a fixed $\mathrm{C_s}$ value in Fig. 4-5(a), while $\mathrm{C_s}$ values that is increased by $(1+\epsilon)$ times were employed in Fig. 4-5(b) to implement the strain effect compensation. In both cases, the OLED efficiency (η) and A were set to 5.3 $\mathrm{cd/A}$, and 250 $\mu\mathrm{m}^2$, respectively. The V_{th} variations were neglected to clearly observe the effect of strain compensation only. Without strain effect compensation,

luminance reduction described in the equation (3-2) occurs as shown in Fig. 4-5(a). The luminance differences between 0% and 15% strain appears up to 46 cd/m^2 without compensation. However, as shown in Fig. 4-5(b), this value decreases to 7.4 cd/m^2 after compensation, demonstrating that the luminance reduction due to display stretching can be prevented by adopting the proposed compensation pixel circuit.

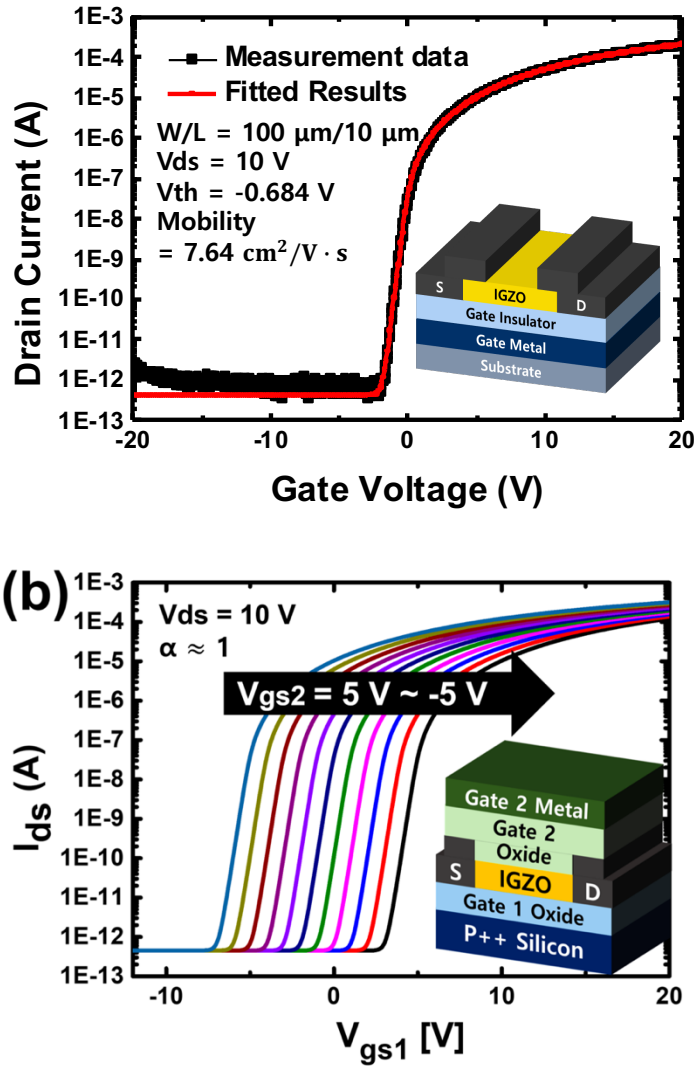

Fig. 4-2. (a) The transfer characteristics of measurement data and fitted results of fabricated IGZO TFT and (b) the simulated transfer curves of the double-gate structure TFT when the V_{gs2} increases from -5 V to 5 V at a 1 V interval.

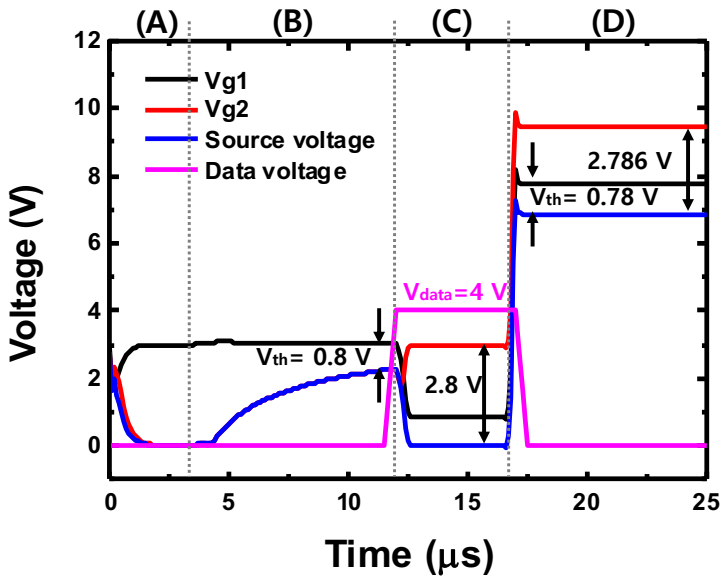

Fig. 4-3. The transient waveform of the data, source, and gate node voltage of T1 in 6T2C circuit with $V_{data} = 4\,V$ without strain.

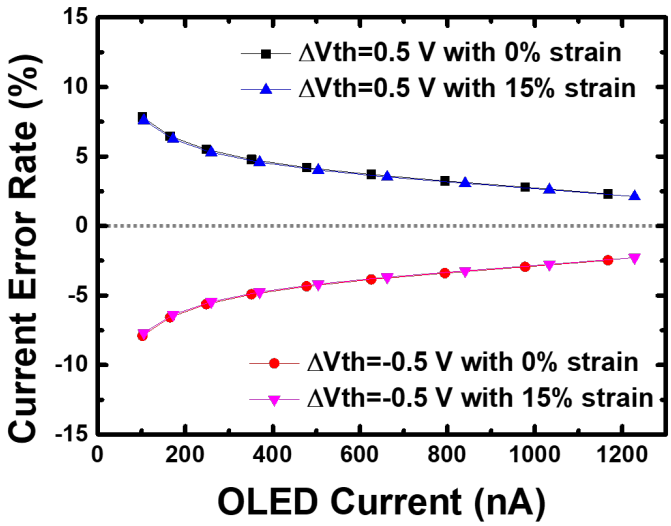

Fig. 4-4. Simulation results of compensation current error rate in 6T2C circuit as a function of the OLED current at 0% and 15% strain.

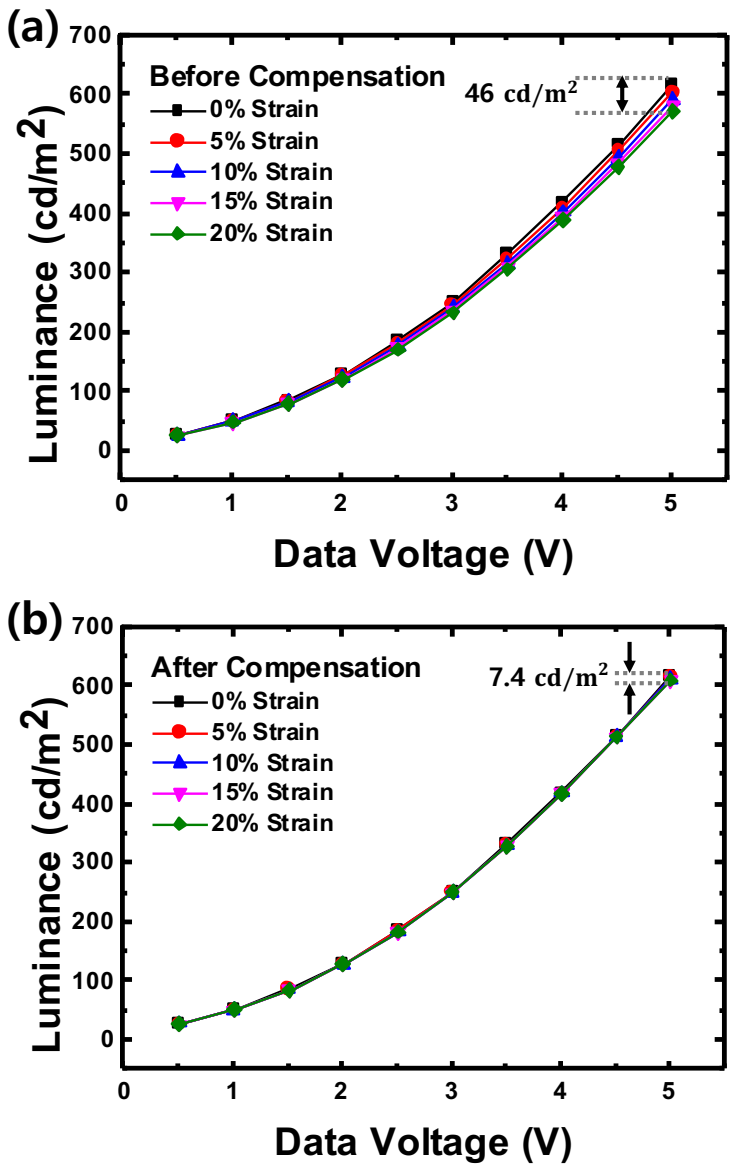

Fig. 4-5. The simulated results of the luminance of the 6T2C circuit are represented as a function of the data voltage at different strains (a) without and (b) with compensation.

4.2. The Proposed 5T2C Pixel Circuit for Stretchable Display

4.2.1. The Operation Principle of the Proposed 5T2C Pixel Circuit

The previous 6T2C pixel circuit uses a double-gate structure TFT as a driving TFT. However, the fabrication process of double-gate structure TFTs is much more complicated than that of single-gate structures [36-37]. Thus, the pixel circuit for the stretchable display that only consists of single-gate structure TFTs is proposed.

Fig. 4-6 shows the schematic of the proposed circuit and the timing diagram of signals. The circuit has 5 TFTs (T1-T5), two storage capacitors (C1, C2), and a capacitive-type strain sensor (Cs). The S1 and S2 signals are adopted to control the switching TFTs. The operation of the proposed circuit is also divided into four stages and the detailed operation principles are described as follows.

(A) Reset Stage

First, the S1 and S2 go high, so that all TFTs are turned on. The source node voltage of T1 and the voltage of node A (V_A) are set to 0 V, and the voltage of node B (V_B) becomes V_{ref}.

(B) V_{th} Compensation Stage

After that, the S1 goes low to turn off T2 and T5. The current

starts to flow through T1 until the voltage between the source and B nodes becomes V_{th} of T1. At the end of this period, V_{th} of T1 is stored at C2.

(C) Data Input Stage

Next, the S2 goes low, turning off T3 and T4 to maintain V_{th} at the C2. At the same time, the S1 rises to a high level so that T2 and T3 are turned on. The data voltage (V_{data}) comes through T2, divided by capacitive coupling of C1 and Cs. Thus, $V_{data}\left(\frac{C_s}{C_1+C_s}\right)$ is stored in C1.

(D) Emission Stage

Finally, as all signals becomes low, all TFTs except for T1 are turned off. The voltage stored in C1 and C2 are maintained as $V_{data}(\frac{C_s}{C_1+C_s})$ and V_{th}, respectively. Thus, V_{gs}, which is equals to the sum of the voltages stored in C1 and C2, can be described as $V_{data}(\frac{C_s}{C_1+C_s}) + V_{th}$, and the OLED current can be defined as follows:

$$I_{OLED} = k(V_{gs} - V_{th})^2 = k\left\{V_{data}\left(\frac{C_s}{C_1 + C_s}\right)\right\}^2 \quad (4-7)$$

where $k = \frac{1}{2}\mu C_{ox}\frac{W}{L}$. Thus, it is demonstrated that the OLED current is not varied by V_{th} of T1. When the strain ϵ is applied on the panel, voltage stored in C1 is changed as $V_{data}\left\{\frac{C_s(1+\epsilon)}{C_1+C_s(1+\epsilon)}\right\}$. By adopting the

equation (3-5), I_{OLED} can increase to $I_{OLED}\{1+(1-\nu)\epsilon\}$, showing that the proposed circuit can effectively compensate for the luminance reduction caused by display stretching.

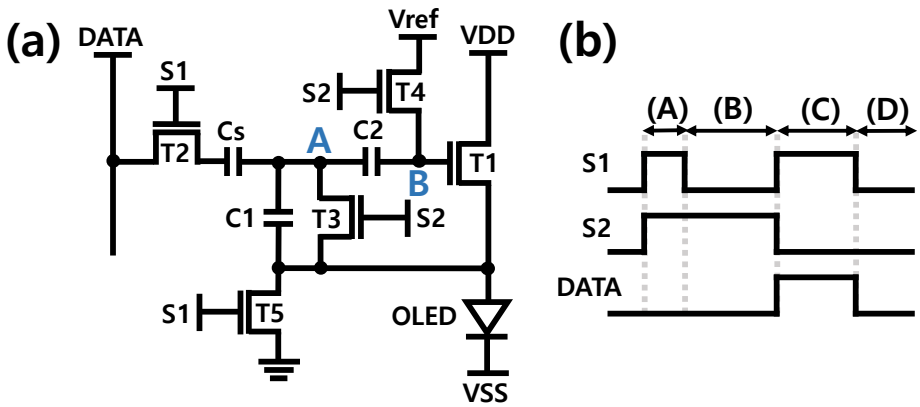

Fig. 4-6. (a) The schematic and (b) the timing diagram of control signals of the proposed 5T2C pixel circuit.

4.3.2. The Simulation Results

Fig. 4-7 shows the transfer characteristics of fabricated single-gate IGZO TFT and fitted data by adjusting the parameters of the level 62 RPI TFT model in HSPICE. The V_{th} and mobility of the fabricated TFT are -0.684 V and 7.64 $cm^2/V\cdot s$, respectively. The design parameters and voltage levels are presented in Table 2. ν was set as 0.5, and the capacitance value were adjusted according to the equation (3-5).

Parameters	Value	Parameters	Value
$\left(\frac{W}{L}\right)_{T1}$	$\frac{15\ \mu m}{5\ \mu m}$	$\left(\frac{W}{L}\right)_{T2-T5}$	$\frac{5\ \mu m}{5\ \mu m}$
C1	300 fF	C2	100 fF
Cs	300 fF	Vref	3 V
VDD	20 V	VSS	2 V
VGH/VGL	20 V/-5 V	Data Voltage	1 V ~ 5 V

Table 2. The design parameters and voltage levels used in 5T2C circuit simulation.

Fig. 4-8 depicts the transient waveform of the A and B nodes, the source node of the T1, and data voltage at 0% strain. As shown in the figure, V_{th} is well detected at the end of the (B) stage. This value is nearly unchanged at the data input (C) and emission (D) stages.

Fig. 4-9 shows the current error rate represented as a function of the OLED current at 0% and 15% strain. V_{th} are shifted by $\pm$ 0.5 V, and the current error rates are calculated using the equation (4-6). The C_s value was increased by 15% to simulate I_{OLED} at 15% strain. As depicted in the figure, the error rate appears within 10% for all cases, verifying that the V_{th} compensation is successfully achieved even under 15% strain is applied.

Fig. 4-10 demonstrates the strain effect compensation capability

of the proposed circuit. The luminance was calculated by the equation (3-1) with A increased by $(1+\epsilon)(1-\nu\epsilon)$ times. I_{OLED} before compensation were simulated with a fixed C_s value, while I_{OLED} after compensation were simulated with $C_s(1+\epsilon)$. The OLED efficiency (η) and A were set to 5.3 cd/A, and 250 μm^2, respectively, and the results are depicted in Fig. 4-10. The threshold voltage variation was excluded for clear observation of the capability of strain effect compensation only. As shown in Fig. 4-10(a), the difference between the luminance at 20% strain and 0% strain appears up to 41.1 cd/m^2 before compensation. This value was reduced to 6.3 cd/m^2 in Fig. 4-10(b), verifying that the luminance reduction can be effectively suppressed with the proposed circuit.

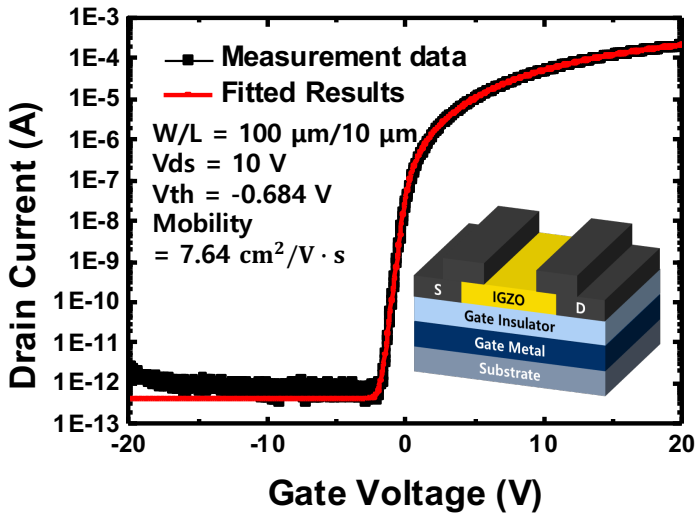

Fig. 4-7. The measured transfer characteristics of the fabricated single-gate structure TFT and fitted results.

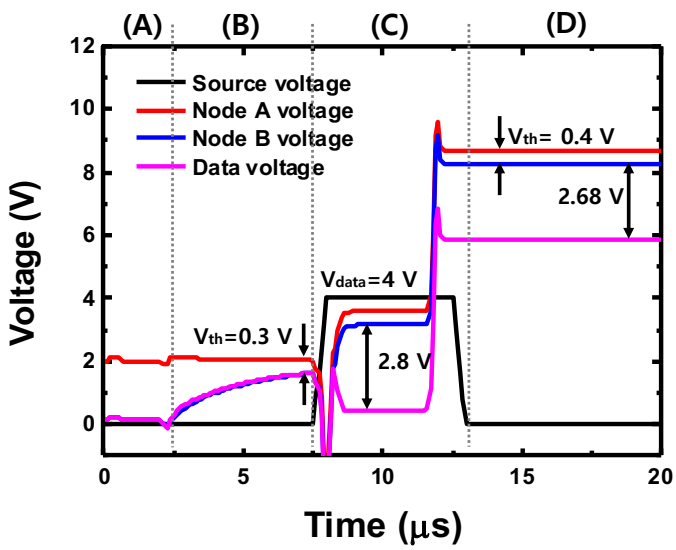

Fig. 4-8. The transient waveform of the data, source, and gate node voltage of T1 in 5T2C circuit with $V_{data} = 4V$ without strain.

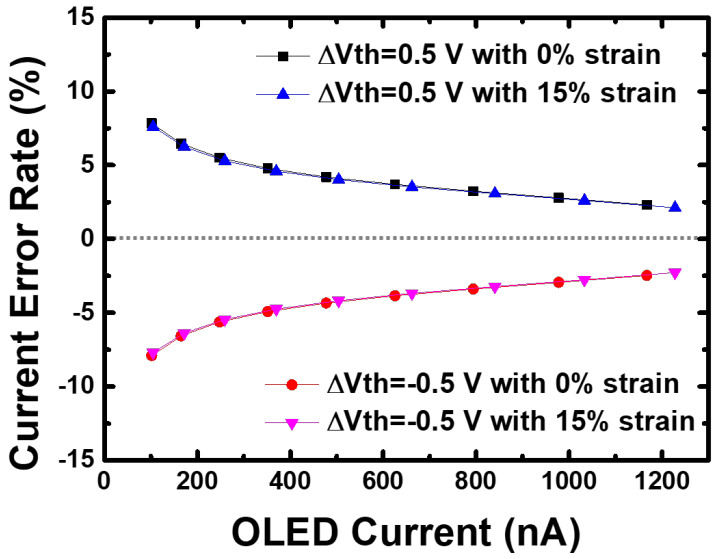

Fig. 4-9. Simulation results of compensation current error rate in 5T2C circuit as a function of the OLED current at 0% and 15% strain.

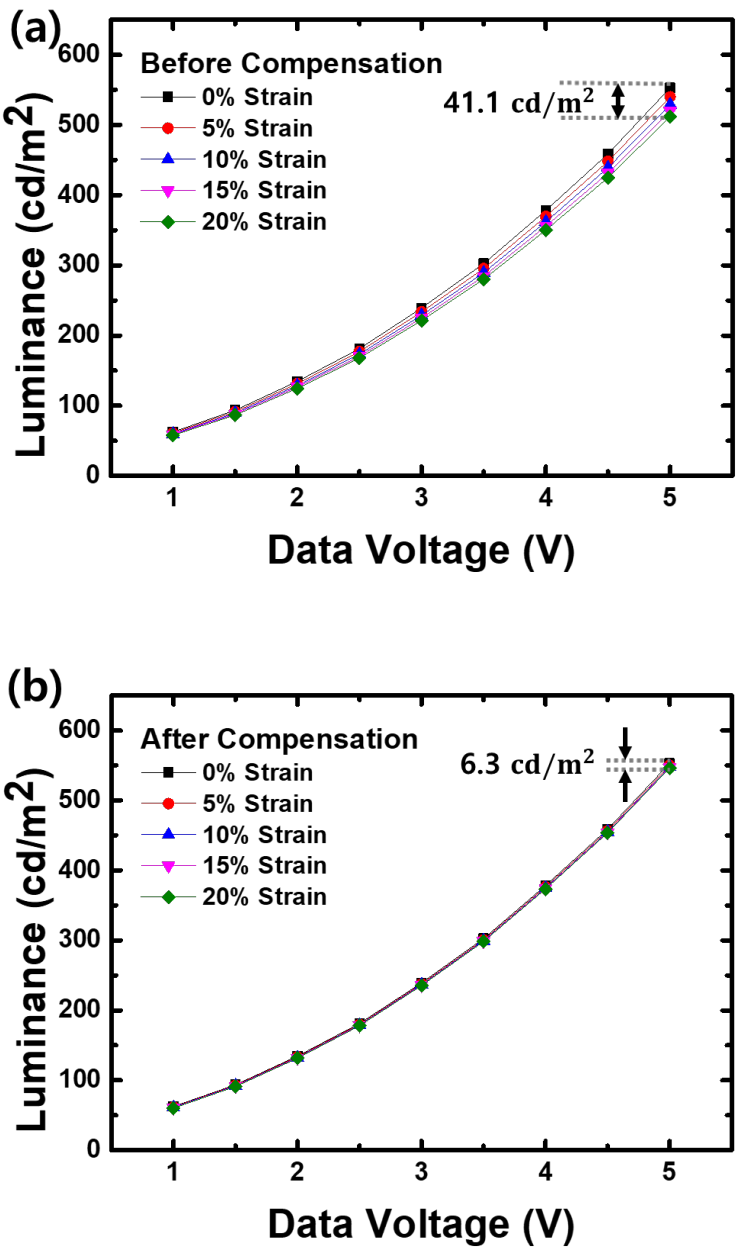

Fig. 4-10. The simulated results of the luminance of the 5T2C circuit at different strain represented as a function of the data voltage at different strain (a) without and (b) with compensation.

4.3. The Proposed 5T1C Pixel Circuit for Stretchable Display

4.3.1. The Operation Principle of the Proposed 5T1C Pixel Circuit

The number of circuit elements in a pixel circuit is crucial in terms of the resolution of the display because the size of pixels decides the resolution. Thus, it is important to reduce the number of pixel elements in the circuit for high-resolution displays. In general, capacitors occupy the most space in the pixel circuit layout. However, reducing the size of the capacitors can increase the leakage, which can degrade the circuit performance [38]. Therefore, the pixel circuit that adopts only one storage capacitor has been proposed in this chapter.

The schematic of the proposed circuit and the timing diagram of signals are shown in Fig. 4-11. The proposed circuit consists of 5 single-gate structure TFTs (T1-T5), 1 storage capacitor (Cst), and 1 capacitive-type strain sensor (Cs). Each frame time is divided into 4 stages: (A) reset, (B) V_{th} compensation, (C) data input, and (D) emission stage. The detailed operation principles are described as follows.

(A) Reset Stage

First, the S1 and S2 go high and turn T2 and T4 on to reset the gate

and source nodes as V_{ref} and 0 V, respectively. The EM2 goes low to turn off T5, cutting off the current flows into the OLED.

(B) V_{th} Compensation Stage

Next, the S2 goes low to turn off T4. Current flows through T1 until V_{th} of T1 is stored at Cst. The stored V_{th} is maintained constant throughout the rest of the frame.

(C) Data Input Stage

After the V_{th} compensation is over, the data voltage (V_{data}) comes through T2. By the capacitive coupling of Cst and Cs, the voltage stored in Cst changes as

$$V_{th} + V_{data}\left(\frac{\mathrm{C_s}}{\mathrm{C_{st}} + \mathrm{C_s}}\right) \tag{4-8}$$

In addition, the EM1 turns off T3 to block the current that flows through T1, preventing the unwanted charging of Cs and Cst.

(D) Emission Stage

Finally, the EM1 and EM2 go high and OLED starts to emit the light. The OLED current can be described as the following equation.

$$I_{OLED} = k\left(V_{gs} - V_{th}\right)^2 = k\left\{V_{data}\left(\frac{\mathrm{C_s}}{\mathrm{C_{st}} + \mathrm{C_s}}\right)\right\}^2 \tag{4-9}$$

where $k = \frac{1}{2}\,\mu C_{ox}\frac{W}{L}$. Thus, V_{th} term can be deleted from this OLED

current equation.

When strain ϵ is applied, the capacitance of the strain sensor increases as $C_s(1+\epsilon)$. Thus, the OLED current will be increased as follows:

$$I_{OLED}\{1+(1-\nu)\epsilon\} = k\left\{V_{data}\left(\frac{C_s}{C_{st}+C_s}\right)\sqrt{1+(1-\nu)\epsilon}\right\}^2 \quad (4-10)$$

Therefore, it is demonstrated that the proposed circuit can compensate for both V_{th} variation and luminance reduction caused by display stretching.

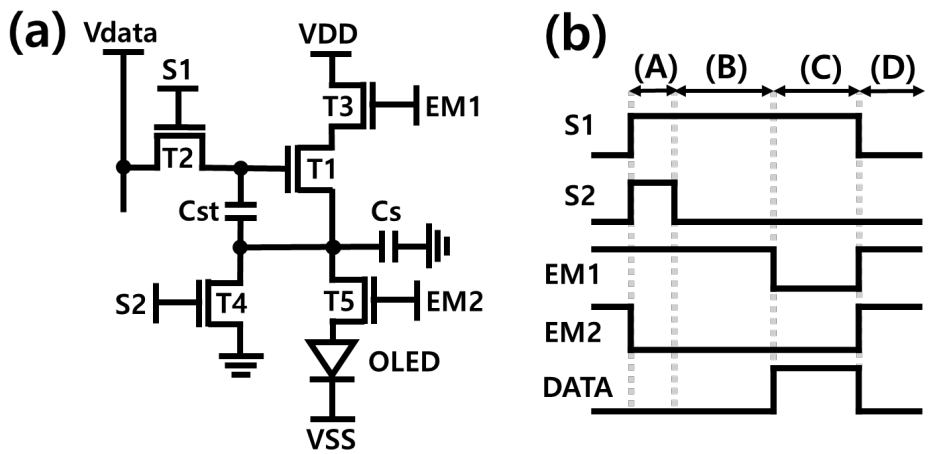

Fig. 4-11. (a) The schematic and (b) the timing diagram of control signals of the proposed 5T1C pixel circuit.

4.3.2. The Simulation Results

The measurement data of transfer characteristics of fabricated single-gate IGZO TFT and the fitted results are depicted in Fig. 4-12. The curves were fitted by the parameters of 62 RPI model in HSPICE. The V_{th} and mobility of the fabricated TFT are -0.684 V and 7.64 $cm^2/V \cdot s$, respectively. The design parameters and the voltage levels are shown in Table 3. ν was set to 0.5, and the capacitance values were adjusted according to the equation (3-5).

Parameters	Value	Parameters	Value
$\left(\frac{W}{L}\right)_{T1}$	$\frac{12\ \mu m}{5\ \mu m}$	$\left(\frac{W}{L}\right)_{T2-T5}$	$\frac{5\ \mu m}{5\ \mu m}$
Cst	100 fF	Cs	300 fF
Vref	3 V	VDD/VSS	20 V/2 V
VGH/VGL	20 V/-5 V	Data Voltage	1 V ~ 4.5 V

Table 3. The design parameters and voltage levels used in 5T1C circuit simulation.

The simulation results of transient waveform of data, gate, and source nodes of T1 are illustrated in Fig. 4-13, when V_{data} is set to 4 V, and strain is not applied. At the data input stage, V_{data} is applied to the gate node of T1, stored and divided by capacitive coupling between

C_s and Cst. The voltage stored in Cst, i.e., V_{gs}, is described as the equation (4-8). Since V_{th} is sensed as 0.7 V, and V_{data} is 4 V, V_{gs} is calculated to be 3.7 V, which closely aligns with the simulated value of 3.67 V. This value remains nearly constant throughout the emission period.

Fig. 4-14 shows the compensation current error rate as a function of the OLED current. V_{th} are shifted by $\pm$ 0.5 V, and the results at 0% and 15% strain are compared. The compensation error rates are calculated by the equation (4-6). The results at 15% strain were simulated with the C_s value increased by 15%. As depicted in the figure, the error rates appear less than 10% in all the cases, demonstrating that the V_{th} are successfully compensated in the proposed circuit and are rarely affected by the strain effect.

Fig. 4-15 depicts the simulated luminance as a function of the data voltage at different strain. The luminance was calculated by the equation (3-1). A was increased by $(1+\epsilon)(1-\nu\epsilon)$ times to indicate the display stretching, and I_{OLED} were simulated with C_s in Fig. 4-15(a), and with $C_s(1+\epsilon)$ in Fig. 4-15(b), respectively. V_{th} are not shifted to clearly show the ability of strain compensation aside from ability of V_{th} compensation. As depicted in Fig. 4-15(a), the luminance at 20%

strain is 43.2 $\mathbf{cd/m^2}$ less than the luminance at 0% strain when V_{data} is 4.5 V, showing the luminance reduction due to the display stretching. However, this difference is decreased to 2.3 $\mathbf{cd/m^2}$ after compensation, indicating that the proposed circuits effectively compensate for the luminance reduction.

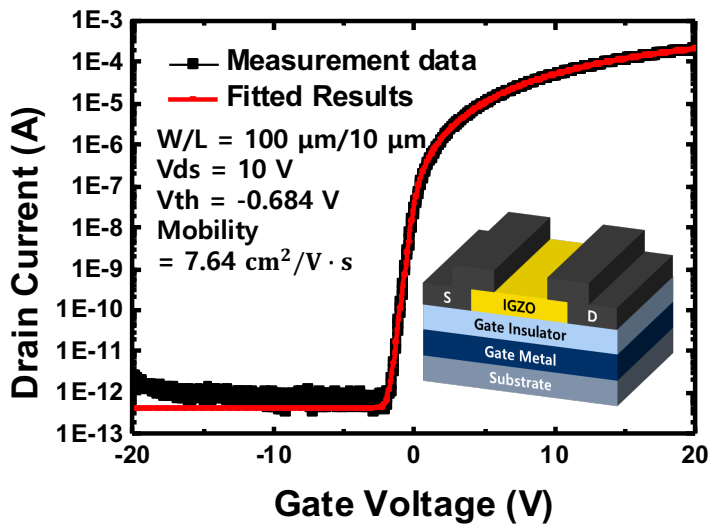

Fig. 4-12. The measured transfer characteristics of the fabricated single-gate structure TFT and fitted results.

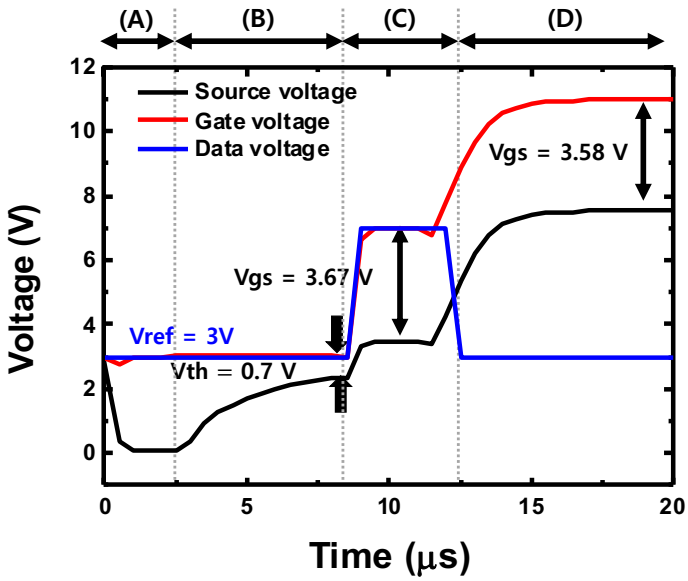

Fig. 4-13. The transient waveform of the data, source, and gate node voltage of T1 in 5T1C circuit with $V_{data} = 4\,V$ without strain.

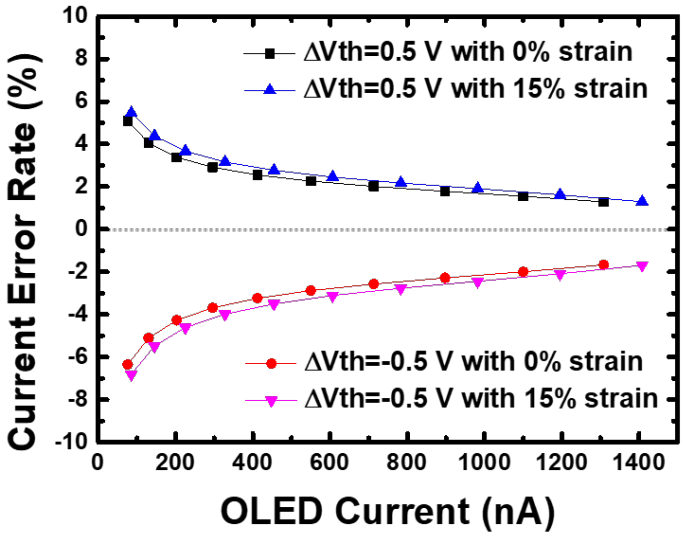

Fig. 4-14. Simulation results of compensation current error rate in 5T1C circuit as a function of the OLED current at 0% and 15% strain.

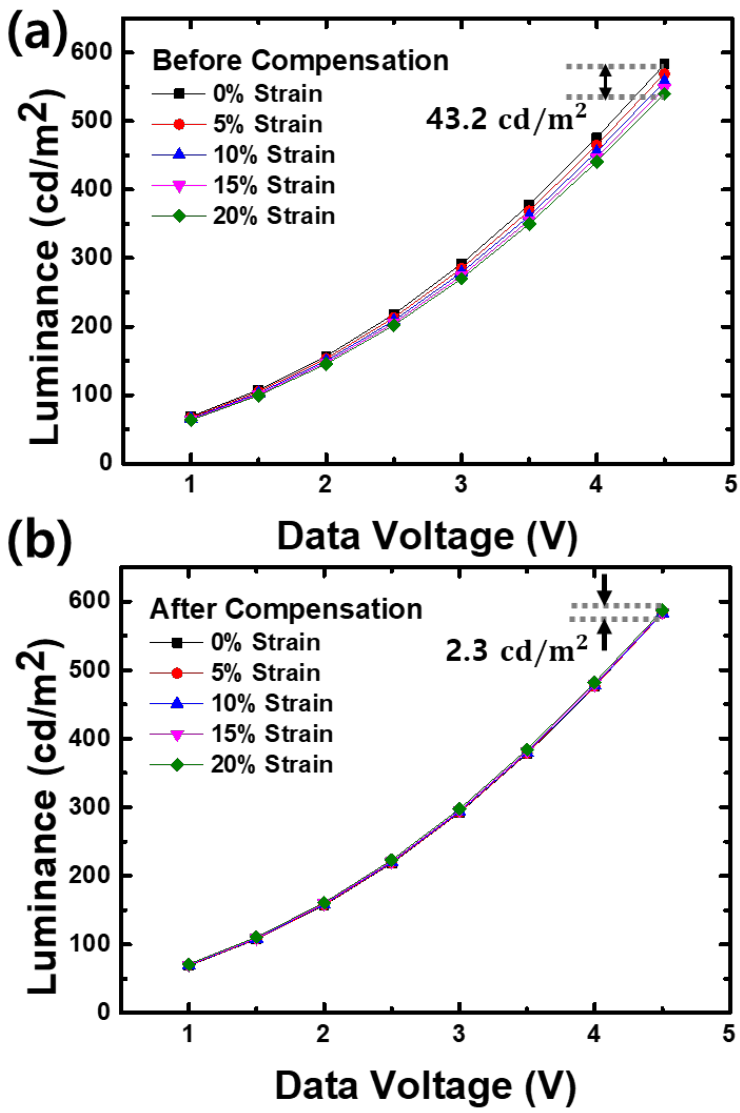

Fig. 4-15. The simulated results of the luminance of 5T1C circuit represented as a function of the data voltage at different strain (a) without and (b) with compensation.

Chapter 5. Conclusion

In this paper, the three novel pixel circuits for the stretchable AMOLED displays have been proposed. All proposed circuits effectively compensate for both threshold voltage variation and luminance reduction caused by display stretching. The source-follower method is utilized to store the negative threshold voltage of the oxide semiconductor TFT. A capacitive-type strain sensor, that can detect the strain by the change of its capacitance, is adopted to compensate for the strain effect.

The first proposed pixel circuit is 6T2C circuit, which exploits a double-gate structure TFT as a driving TFT. By adopting the double-gate structure property, the threshold voltage compensation is held at the first gate, and the data input and strain effect compensation are held at the second gate with the capacitive-type sensor. However, this structure requires more fabrication steps than the single gate structure, so the 5T2C pixel circuit, that is only composed of single-gate structure TFTs, is also proposed.

To reduce the pixel area, the 5T1C circuit is proposed, which utilizes only one storage capacitor to compensate for both threshold

voltage and luminance reduction. The capacitor size is not decreased to prevent unexpected leakage that could increase the compensation error rate.

SPICE simulation is used to demonstrate the performance and compensation ability of the proposed circuits. In all cases, the current error rates of the proposed circuits are less than 10%, indicating effective compensation for the threshold voltage variations of the driving transistor. Furthermore, such error rates show almost the same when the 15% strain is applied, showing that the proposed circuits can stably operate under the strain.

In addition, the luminance of the display at the different strain and data voltage were calculated by the simulated OLED currents. The significant luminance reductions due to the display stretching were observed without compensation. After introducing the compensation, the luminance differences according to the strain were effectively suppressed, indicating that the proposed circuit compensate for the strain effect of the stretchable display. The simulation results verify that the proposed pixel circuits contribute to the improvement of image quality in stretchable AMOLED displays.

Bibliography

[1] Kim, Hye Dong, et al. "Emerging technologies for the commercialization of AMOLED TVs." Information Display 25.9 (2009): 18-22.

[2] Arai, Toshiaki. "Oxide-TFT technologies for next-generation AMOLED displays." Journal of the Society for Information Display 20.3 (2012): 156-161.

[3] Nomura, Kenji, et al. "Room-temperature fabrication of transparent flexible thin-film transistors using amorphous oxide semiconductors." nature 432.7016 (2004): 488-492.

[4] Park, Joon Seok, et al. "Review of recent developments in amorphous oxide semiconductor thin-film transistor devices." Thin solid films 520.6 (2012): 1679-1693.

[5] Yabuta, Hisato, et al. "High-mobility thin-film transistor with amorphous InGaZnO4 channel fabricated by room temperature rf-magnetron sputtering." Applied physics letters 89.11 (2006): 112123.

[6] In, Hai-Jung, and Oh-Kyong Kwon. "External compensation of nonuniform electrical characteristics of thin-film transistors and degradation of OLED devices in AMOLED displays." IEEE Electron Device Letters 30.4 (2009): 377-379.

[7] Lee, Kuei-Yu, et al. "A new compensation method for emission degradation in an AMOLED display via an external algorithm, new pixel circuit, and models of prior measurements." Journal of display technology 10.3 (2013): 189-197.

[8] Wu, Wei-Jing, et al. "A new voltage-programmed pixel circuit for enhancing the uniformity of AMOLED displays." IEEE Electron Device Letters 32.7 (2011): 931-933.

[9] Lin, Chih-Lung, Wen-Yen Chang, and Chia-Che Hung. "Compensating pixel circuit driving AMOLED display with a-IGZO TFTs." IEEE electron device letters 34.9 (2013): 1166-1168.

[10] Lin, Chih-Lung, et al. "Compensation pixel circuit to improve image quality for mobile AMOLED displays." IEEE Journal of Solid-State Circuits 54.2 (2018): 489-500.

[11] Koo, Ja Hoon, et al. "Flexible and stretchable smart display: materials, fabrication, device design, and system integration." Advanced Functional Materials 28.35 (2018): 1801834.

[12] Hong, Jong-Ho, et al. "9.1-inch stretchable AMOLED display based on LTPS technology." Journal of the Society for Information Display 25.3 (2017): 194-199.

[13] Lee, Yeongjun, et al. "Advancements in Electronic Materials

and Devices for Stretchable Displays." Advanced Materials Technologies (2023): 2201067.

[14] Liang, Jiajie, et al. "Intrinsically stretchable and transparent thin-film transistors based on printable silver nanowires, carbon nanotubes and an elastomeric dielectric." Nature communications 6.1 (2015): 7647.

[15] Liu, Yuan, et al. "Capillary-force-induced cold welding in silver-nanowire-based flexible transparent electrodes." Nano letters 17.2 (2017): 1090-1096.

[16] Hong, Soo Yeong, et al. "High-Sensitivity, Skin-Attachable, and Stretchable Array of Thermo-Responsive Suspended Gate Field-Effect Transistors with Thermochromic Display." Advanced Functional Materials 29.6 (2019): 1807679.

[17] Hong, Jong-Ho, et al. "9.1-inch stretchable AMOLED display based on LTPS technology." Journal of the Society for Information Display 25.3 (2017): 194-199.

[18] Jablonski, Michal, et al. "Impact of geometry on stretchable meandered interconnect uniaxial tensile extension fatigue reliability." Microelectronics Reliability 55.1 (2015): 143-154.

[19] Cho, Hyeon, et al. "Recent progress in strain-engineered

elastic platforms for stretchable thin-film devices." Materials Horizons (2022).

[20] Silva, Cristian A., et al. "Liquid metal based island-bridge architectures for all printed stretchable electrochemical devices." Advanced Functional Materials 30.30 (2020): 2002041.

[21] Sim, Kyoseung, et al. "Biaxially stretchable ultrathin Si enabled by serpentine structures on prestrained elastomers." Advanced Materials Technologies 4.1 (2019): 1800489.

[22] Miyakawa, Masashi, Hiroshi Tsuji, and Mitsuru Nakata. "Highly stretchable island-structure metal oxide thin-film transistor arrays using acrylic adhesive for deformable display applications." Journal of the Society for Information Display 30.9 (2022): 699-705.

[23] Han, Ki-Lim, et al. "Mechanical durability of flexible/stretchable a-IGZO TFTs on PI island for wearable electronic application." ACS Applied Electronic Materials 3.11 (2021): 5037-5047.

[24] Amjadi, Morteza, et al. "Stretchable, skin-mountable, and wearable strain sensors and their potential applications: a review." Advanced Functional Materials 26.11 (2016): 1678-1698.

[25] Wang, Yalong, et al. "Flexible electrically resistive-type strain

sensors based on reduced graphene oxide-decorated electrospun polymer fibrous mats for human motion monitoring." Carbon 126 (2018): 360-371.

[26] Wu, Yu-Ting, Tao Yan, and Zhi-Juan Pan. "Wearable carbon-based resistive sensors for strain detection: a review." IEEE Sensors Journal 21.4 (2020): 4030-4043.

[27] Obitayo, Waris, and Tao Liu. "A review: Carbon nanotube-based piezoresistive strain sensors." Journal of Sensors 2012 (2012).

[28] Zhao, Jing, Guang-Yu Zhang, and Dong-Xia Shi. "Review of graphene-based strain sensors." Chinese Physics B 22.5 (2013): 057701.

[29] Nur, Roda, et al. "A highly sensitive capacitive-type strain sensor using wrinkled ultrathin gold films." Nano letters 18.9 (2018): 5610-5617.

[30] Kim, Seung-Rok, Jin-Hoon Kim, and Jin-Woo Park. "Wearable and transparent capacitive strain sensor with high sensitivity based on patterned Ag nanowire networks." ACS applied materials & interfaces 9.31 (2017): 26407-26416.

[31] Nesser, Hussein, and Gilles Lubineau. "Strain sensing by electrical capacitive variation: From stretchable materials to

electronic interfaces." Advanced Electronic Materials 7.10 (2021): 2100190.

[32] Jeon, Chang Hoon, et al. "Fast threshold voltage compensation AMOLED pixel circuit using secondary gate effect of dual gate a-IGZO TFTs." IEEE Electron Device Letters 37.11 (2016): 1450-1453.

[33] Chou, Lu-Sheng, et al. "56.4: Dual-Gate IGZO TFT for Threshold-Voltage Compensation in AMOLED Pixel Circuit." SID Symposium Digest of Technical Papers. Vol. 43. No. 1. Oxford, UK: Blackwell Publishing Ltd, 2012.

[34] Tai, Ya-Hsiang, et al. "Three-transistor AMOLED pixel circuit with threshold voltage compensation function using dual-gate IGZO TFT." IEEE electron device letters 33.3 (2012): 393-395.

[35] S. K. Dargar and V. M. Srivastava, "Design of Double-Gate Tri-Active Layer Channel Based IGZO Thin-Film Transistor for Improved Performance of Ultra-Low-Power RFID Rectifier," in IEEE Access, vol. 8, pp. 194652-194662, 2020, doi: 10.1109/ACCESS.2020.3034031.

[36] Rahaman, Abidur, et al. "A high performance operational amplifier using coplanar dual gate a-IGZO TFTs." IEEE Journal of the Electron Devices Society 7 (2019): 655-661.

[37] Li, Xiuling, et al. "High-speed dual-gate a-IGZO TFT-based circuits with top-gate offset structure." IEEE Electron Device Letters 35.4 (2014): 461-463.

[38] Lin, Chih-Lung, et al. "Pixel circuit with leakage prevention scheme for low-frame-rate AMOLED displays." IEEE Journal of the Electron Devices Society 8 (2020): 235-240.

Appendix. The Fabrication Process of Devices

The single-gate structure IGZO TFT was fabricated according to the following process. First, a boron-doped silicon substrate with 200nm dry oxidization layer was cleaned. Next, 40 nm IGZO was deposited as a channel layer by RF magnetron sputtering. The gas pressure, Ar/O_2 flow rate, and RF power were 6 mTorr, 50/1 sccm, and 100 W, respectively. Then, the channel layer was patterned by photolithography process and wet etching. After that, 70 nm Ti layer was deposited by e-beam evaporator and lifted-off to form a source and drain electrodes. Finally, the device was annealed at 300 ℃ for 30 minutes in the air atmosphere. Fig. A shows the overall fabrication process flow and structure of the fabricated IGZO TFT.

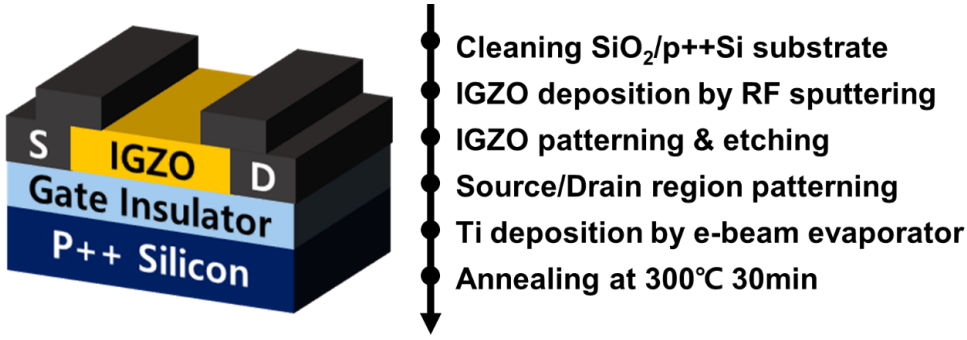

Fig. A. The structure and the fabrication process flow of the single-gate structure IGZO TFT.

초록

최근, 모양과 크기가 자유자재로 변형될 수 있는 스트레처블 디스플레이가 변형 가능한 디스플레이의 궁극적인 형태로서 주목받고 있다. 현재까지 스트레처블 디스플레이에 대한 연구는 기계적인 스트레스가 인가될 때도 안정적으로 동작될 수 있는 방법에 대한 연구가 주를 이루고 있다. 대표적으로, 디스플레이 소자들에 직접적으로 가해지는 변형을 완화시켜 줄 수 있는 rigid-island 구조가 널리 사용되고 있다. 그러나 이러한 구조가 변형으로 인한 디스플레이 소자의 열화를 최소화할 수 있음에도 불구하고, 디스플레이 이미지 화질 문제는 여전히 존재한다. 디스플레이의 밝기는 픽셀의 면적에 반비례하는데, 디스플레이가 신장됨에 따라, 픽셀의 면적이 증가하게 된다. 따라서, 디스플레이 신장 시 필연적으로 밝기가 감소하게 된다.

지금껏, 평판 능동 구동 유기 발광 다이오드 (AMOLED) 디스플레이는 높은 균일도를 가지는 고화질 이미지를 얻기 위해 보상 기술을 사용해왔다. 보상 회로는 구동 박막 트랜지스터의 문턱 전압 변동을 보상하여 디스플레이 이미지 열화를 방지할 수 있다.

본 논문에서는 rigid-island 구조의 스트레처블 AMOLED 디스플레이용 화소 보상 회로들을 제안한다. 제안된 화소 보상 회로들은 구동 박막 트랜지스터의 문턱 전압을 보상할 뿐만 아니라, 저장 용량 방식의 변형 센서를 도입하여 디스플레이 신장에 의한 밝기 감소 문제를 해결한다. 디스플레이 신장에 의한 밝기 감소를 보상하기 위한 방법으로 변형 센서와 스트레인 사이의 선형적인 관계가 이용된다. 제안된 회로를 통해 스트레처블 디스플레이의 화질 열화 문제를 개선할 수 있다.

각 화소 회로들의 동작과 보상 오차는 SPICE 시뮬레이션을 통해 검증되었다. 문턱 전압 변동에 의한 보상 오차는 신장 시에도 10% 이하로 나타나며 우수한 보상 능력을 보였으며, 신장에 의한 밝기 감소 또한 보상 이후 확연히 감소한 것을 관찰할 수 있었다. 시뮬레이션 결과로 제안된 화소 회로들이 문턱 전압 변동과 신장에 의한 밝기 감소를 효과적으로 보상함을 검증할 수 있었다.

결론적으로, 이 논문에서 제안하는 화소 회로는 스트레처블 디스플레이의 문제를 해결할 수 있는 새로운 방안을 제시하며, 스트레처블 디스플레이의 화질 개선 가능성을 보여준다.

주요어 : 스트레처블 디스플레이, AMOLED 디스플레이, 픽셀 회로, 보상, 변형 센서, rigid-island 구조
학번 : 2021-29608